High-performance neural prosthetic control along instructed paths

Patrick T. Sadtler, *Student Member, IEEE*, Stephen I. Ryu, Byron M. Yu, and Aaron P. Batista

Abstract—Neural prostheses are becoming increasingly feasible as assistive technologies for paralyzed patients. A major goal is to provide control of a prosthesis rivaling the natural arm in speed, accuracy, and flexibility. Here, we demonstrate high-performance cursor control by training a monkey to move a cursor in a 2D virtual reality environment using neural activity recorded in primary motor cortex. On a standard center-out task with 8 possible targets, the subject maintained a success rate greater than 95% over many hundreds of trials, on par with previous reports. We introduced the more challenging task of moving the cursor along instructed paths with zero, one, and two inflections. Over several weeks, the subject's performance with double-inflection paths reached a stable level of greater than 55% success with movement times approaching those of the natural arm. Our instructed trajectory task provides a new standard for quantification of prosthesis performance: since the subject's intended movement is known (i.e. the instructed path), we can compute the root mean-square-error (RMSE) between the decoded and intended cursor position throughout the reach. We found that, while success rate tended to increase with training, the RMSE among successful trials remained largely unchanged, consistent with the all-or-none reward scheme. In sum, this work demonstrates the utility of instructed paths for i) pushing the limits of the subject's control and ii) rigorously quantifying the accuracy of cursor movements, both of which are critical for increasing the clinical viability of neural prosthetic systems.

I. INTRODUCTION

NEURAL PROSTHESES aim to assist paralyzed patients by translating neural activity into movements of a computer cursor or prosthetic limb. Previous studies have demonstrated that subjects are able to use neural activity to guide a cursor or limb to a desired endpoint [1]–[3]. A major challenge is to develop prostheses that rival the natural limb in speed, accuracy, and flexibility. To this end, we must push the limits of the subject's control of the prosthesis, in addition to more rigorously quantifying performance beyond

endpoint accuracy and movement time [4]. Furthermore, in natural arm movements, the trajectory is often as important as the endpoint of the movement [5]. Examples include reaching in cluttered environments, driving, and conversing with sign language.

We developed a novel *instructed trajectory* task in which the subject must steer a prosthetic cursor along a specified path. Movement outside a narrow window around this path was considered a failure. By increasing the number of inflections of the instructed path and/or decreasing the size of the acceptance window around the path, we can increase the difficulty of the task. This allows us not only to probe the limits of the subject's control, but also to challenge the subject to increase its control accuracy. Since the subject's intended movement is known, we can compute the RMSE between the decoded and intended cursor position throughout the reach. To our knowledge, this work provides the first demonstration of cursor control along instructed paths in a closed-loop neural prosthetic setting.

Section II details the neural recordings, instructed trajectory task, and modified Kalman filter used to decode cursor movements from neural activity. Section III describes the closed-loop experimental results for both the endpoint and instructed trajectory tasks. For both tasks, prosthesis performance will be compared to the subject's performance using its natural limb in the same task.

II. METHODS

A. Neural Recordings

Animal protocols were approved by the University of Pittsburgh Institutional Animal Care and Use Committee. A 96-channel electrode array (Blackrock Microsystems, Salt Lake City, UT) was implanted in the primary motor cortex of a male Rhesus monkey (*Macaca mulatta*), contralateral to the reaching arm. Spike sorting was performed by an automated procedure using OpenProject (Tucker-Davis Technologies, Inc., Alachua, FL). Briefly, for each channel, waveforms that exceeded 3.5x the RMS voltage were analyzed using Principal Components Analysis. K-means was used to separate the first three principal components of each channel into two clusters, each of which could be a single-neuron unit or a multi-neuron unit. All clusters were used for decoding regardless of isolation quality.
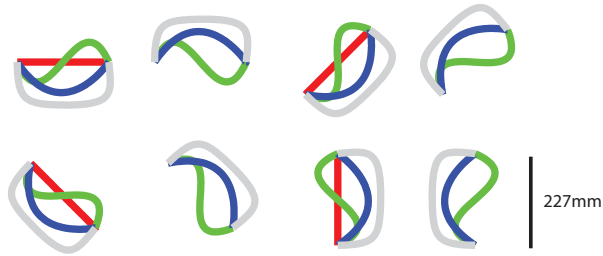
Fig. 1. The 28 possible instructed paths, each of which could be traversed in two directions. The center of each panel corresponds to the center of the monkey's workspace; we split the paths into 8 panels and color-coded the paths for clarity only. All paths were shown in green to the monkey.

B. Behavioral Task

The monkey was trained to perform an endpoint task and an instructed trajectory task by moving a cursor in a 2D virtual reality environment using either its hand (hand control) or its neural activity (brain control). During brain control, the monkey was allowed to move its unrestrained reaching arm. Hand position was tracked using LED sensors (PhaseSpace, Inc., San Leandro, CA).

For the endpoint task, each trial began with the presentation of a central target. Upon acquisition of the target with the cursor, one of 8 peripheral targets (127 mm from the center; separated by 45°) appeared. The monkey then moved the cursor to the peripheral target to receive a juice reward. This is identical to the commonly-used "center-out" task, but no hold period was required.

The instructed trajectory task began with the appearance of one of eight possible start targets (separated by 45°). After the monkey moved the cursor to the start target, an instructed path appeared. The monkey guided the cursor through the path in order to receive a juice reward (successful trial). If the center of the cursor was more than 35 mm from the center of the path at any time after acquiring the start target and before completing the reach, the trial aborted (unsuccessful trial). The straight-line distance from the start to the end of the path was 227 mm; the path length varied depending on the shape of path. There were four types of paths, as shown in Fig. 1: straight, single-inflection, double-inflection, and U-shaped. These paths spanned the monkey's full reaching workspace. With 28 possible instructed paths and two traversal directions for each, there were a total of 56 trial conditions.

At the beginning of each session, the monkey performed ∼100 hand control trials, chosen pseudorandomly from all 56 trial conditions. These trials were used to fit the parameters of the modified Kalman filter described below. Then, the cursor was switched to brain control. In a typical brain control session, we presented only endpoint trials, only straight paths, only single-inflection paths, or only double-inflection paths. In this paper, we focus on the endpoint trials and double-inflection paths, which were the most difficult instructed paths that we tested. Fig. 2 shows the neural activity and cursor path for one typical brain control trial. We also conducted sessions with hand control exclusively.
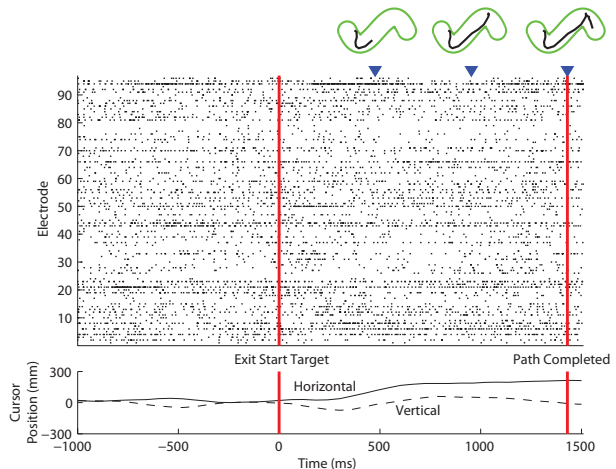

Fig. 2. Neural activity (middle panel) and cursor movement (black lines in upper and lower panels) along a double-inflection path for one representative trial under brain control. Green outline indicates the acceptance window of the instructed path. Blue triangles indicate the times at which each snapshot of the cursor trajectory is taken. [J20101106.844]

For the endpoint task, movement time was measured from when the cursor left the central target to when it arrived at the peripheral target. For the instructed trajectory task, movement time was measured from when the cursor left the start target to when it arrived at the end of the path. RMSE was calculated by finding the square root of the average squared distance between the cursor and the closest point along the center of the instructed path at each timepoint. Percent correct and RMSE timelines in Fig. 6 were smoothed using a boxcar filter across 200 trials.

C. Decoding Methods

During the brain control phase, neural signals were decoded into cursor movements using a modified Kalman filter. We first reduced the dimensionality of the neural data using factor analysis (FA)

$$\mathbf{z} \sim \mathcal{N}\left(\mathbf{0},\, I\right) \tag{1}$$

$$\mathbf{y} \mid \mathbf{z} \sim \mathcal{N}\left(\Lambda \mathbf{z} + \boldsymbol{\mu},\, \Psi\right), \tag{2}$$

where $\mathbf{y} \in \mathbb{R}^{q \times 1}$ is a vector of spike counts taken in 60 ms bins across the q simultaneously-recorded units, and $\mathbf{z} \in \mathbb{R}^{p \times 1}$ contains the p latent factors. Unlike principal components analysis, FA allows each unit to have a different noise variance (Ψ). Each latent factor can be understood as a well-modulated pattern of neural activity across the recorded units. In this work, we set $p = 10$. The parameters $\Lambda \in \mathbb{R}^{q \times p}$, $\boldsymbol{\mu} \in \mathbb{R}^{q \times 1}$, and diagonal covariance $\Psi \in \mathbb{R}^{q \times q}$ were fit using the expectation-maximization algorithm.

We then used a Kalman filter [6] to relate the estimated latent factors at each timepoint $\mathbf{z}_t = E[\mathbf{z} \mid \mathbf{y}]$ to the cursor kinematics $\mathbf{x}_t \in \mathbb{R}^{r \times 1}$, which included position, velocity, and acceleration in the horizontal and vertical directions ($r = 6$).
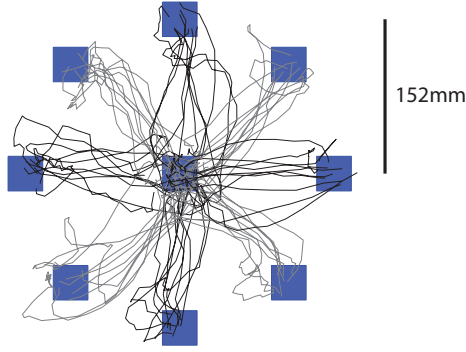
Fig. 3. Sample cursor trajectories for endpoint task under brain control. The colors of the trajectories are only for clarity. [J20110105]

The Kalman filter is described by

$$\mathbf{x}_t \mid \mathbf{x}_{t-1} \sim \mathcal{N}\left(A\mathbf{x}_{t-1},\, Q\right) \qquad (3)$$

$$\mathbf{z}_t \mid \mathbf{x}_t \sim \mathcal{N}\left(C\mathbf{x}_t + \mathbf{d},\, R\right), \qquad (4)$$

where the parameters $A \in \mathbb{R}^{r \times r}$, $Q \in \mathbb{R}^{r \times r}$, $C \in \mathbb{R}^{p \times r}$, $\mathbf{d} \in \mathbb{R}^{p \times 1}$, $R \in \mathbb{R}^{p \times p}$ are fit using maximum likelihood [6]. The position estimate in $E[\mathbf{x}_t \mid \mathbf{z}_1, \ldots, \mathbf{z}_t]$ determines the cursor position shown to the monkey.

Preconditioning the neural data using FA restricts the Kalman filter to associate cursor movements with only the best-modulated patterns of neural activity, even if they are not the patterns that correlate most highly with kinematics. We believe that there are advantages to this approach in a closed-loop prosthetic setting involving the subject's ability to learn, which will be explored in future work.

III. RESULTS

To baseline our work with instructed paths, we performed experiments with a standard endpoint task. Fig. 3 shows sample cursor trajectories under brain control, which are reliably directed towards the instructed endpoint. The monkey was able to succeed with greater than 95% accuracy across many hundreds of trials. Fig. 4 compares the movement times under hand and brain control. Although movement times under brain control (mean: 863 ms) were longer than under hand control (mean: 545 ms), the histograms were almost entirely overlapping, indicating how similar brain control was to hand control.

To challenge the monkey to increase its control accuracy, we introduced instructed paths. We presented the different path types in separate sessions. Over the course of several weeks, the monkey improved its level of control as we gradually increased the task difficulty by increasing the number of path inflections and by decreasing the size of the acceptance window around the path. Here, we focus on the performance for double-inflection paths after this learning period. Fig. 5 shows sample successful cursor paths under hand and brain control. The subject was able to carry out smooth and natural-looking cursor movements under brain control, reminiscent of those under hand control.
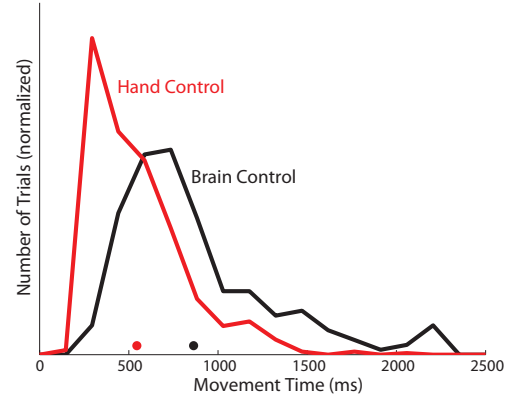

Fig. 4. Movement time histograms for the endpoint task under hand control (red) and brain control (black). Dots indicate distribution means. The distributions were normalized for visual clarity (hand control: 675 trials [J20110112]; brain control: 206 trials [J20110105]) by setting the area under the distributions equal to 1.0.

We quantified these movements by computing a running average of the success rate and RMSE. A representative session is shown in Fig. 6. The success rate on this demanding task increased from around 30% to 50% during the first 300 trials, then increased to over 55% during the remainder of the session. On the same task under hand control, the monkey's success rate was 85%. We also computed the RMSE of the cursor movements among only successful trials. This performance metric was enabled by the use of instructed paths. We found that, although success rate increased during the session, the RMSE stayed flat at around 15 mm. This is consistent with the all-or-none reward scheme. Namely, the monkey was rewarded solely based on whether the cursor traversed the instructed path sucessfully. We did not, for example, give a larger reward on successful trials with lower RMSE. Although the RMSE under brain control was larger than under hand control (12.7 mm), it was far closer to hand control than to the maximum RMSE for the acceptance window size used (35 mm). We also compared the movement times for double-inflection paths under hand and brain control. We found that, although movement times under brain control (mean: 1259 ms) were longer than under hand control (mean: 865 ms), their distributions had substantial overlap, as shown in Fig. 7.

IV. DISCUSSION

In this work, we have demonstrated the utility of instructed trajectories for i) challenging subjects to increase their cursor control accuracy and ii) rigorously quantifying the decoded cursor movements in terms of RMSE, both of which are critical for increasing the clinical viability of neural prosthetic systems. By using instructed paths, we have achieved a level of cursor control that approaches the subject's performance with its natural limb, as measured by success rate, RMSE, and movement time.

Nevertheless, there is still a substantial performance difference between cursor control and movement of the natural limb, and further work will continue to close the gap.
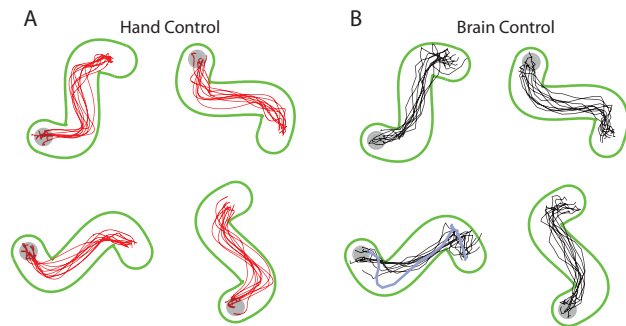
Fig. 5. Sample cursor trajectories for instructed paths. (A) Hand control trajectories for 4 of the 16 double-inflection paths. The gray dots indicate the start of the path. [J20110112] (B) Brain control trajectories for the same paths. The blue trajectory in the bottom left panel corresponds to the trial shown in Figure 2. [J20101106]
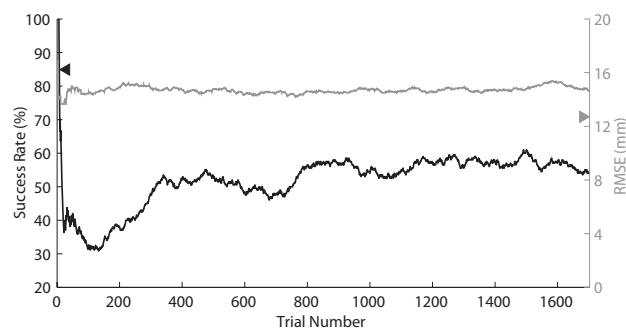

Fig. 6. Success rate (black curve) and RMSE (gray curve) during a representative session with double-inflection paths under brain control. [J20101106] For comparison, success rate (black triangle) and RMSE (gray triangle) for the same task under hand control are also shown. [J20110112]
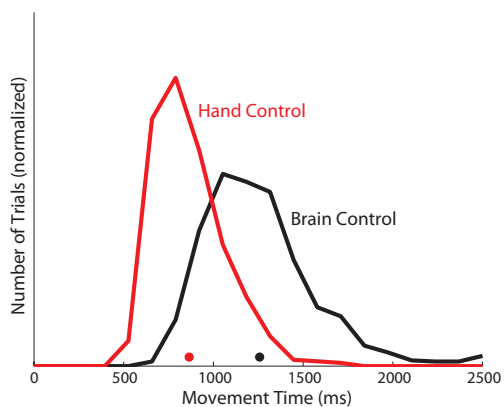

Fig. 7. Movement time histograms for instructed trajectory task under hand control (red) and brain control (black). Dots indicate distribution means. The distributions were normalized for visual clarity (hand control: 642 trials [J20110112]; brain control: 895 trials [J20101106]) by setting the area under the distributions to 1.0.

Recent work has shown that subjects can accurately move a prosthetic cursor around visual barriers to acquire targets [7]. Although that task does not allow for measurement of RMSE, it complements the instructed trajectory task by

demonstrating obstacle avoidance. Another related approach is the "pursuit tracking" task, where the objective is to track a target that moves according to a random walk [4], [6] . This task allows for measurement of RMSE, but to our knowledge, it has not yet been tested in a closed-loop setting. Importantly, all of these tasks allow the experimenter to specify details of the movement trajectory beyond the desired endpoint and to push the limits of the subject's control.

We fit the decoder parameters using hand-control data from all path types (i.e., we used all 56 trial conditions in the first ∼100 trials of each session), regardless of which path type(s) were to be tested under brain control. We found that fitting using a wide variety of paths led to higher brain control performance, presumably because the movements more thoroughly sampled the kinematic space (i.e., the combined space of position, velocity, and acceleration) [4], [6].

There are several future directions for this work. First, although our preliminary results indicate that the Kalman filter with FA preconditioning outperforms the standard Kalman filter, we plan to perform a systematic performance comparison. In this comparison, we will sweep the number of latent factors used by FA. Second, we seek to understand the relationship between the Kalman filter with FA preconditioning and the Kalman filter with hidden states [8]. Third, we plan to conduct experiments with a graded reward scheme to encourage the subject to improve its RMSE during a session.

REFERENCES

[1] M. Velliste, S. Perel, M. D. Spalding, A. S. Whitford, and A. B. Schwartz, "Cortical control of a prosthetic arm for self-feeding," *Nature*, vol. 453, pp. 1098–1101, June 2008.
[2] L. R. Hochberg, M. D. Serruya, G. M. Friehs, J. A. Mukand, M. Saleh, A. H. Caplan, A. Branner, D. Chen, R. D. Penn, and J. P. Donoghue, "Neuronal ensemble control of prosthetic devices by a human with tetraplegia," *Nature*, vol. 443, pp. 164–171, July 2006.
[3] J. M. Carmena, M. A. Lebedev, R. E. Crist, J. E. O'Doherty, D. M. Santucci, D. F. Dimitrov, P. G. Patil, C. S. Henriquez, and M. A. L. Nicolelis, "Learning to control a brain-machine interface for reaching and grasping by primates," *PLoS Biology*, vol. 1, no. 2, pp. 193–208, 2003.
[4] S. P. Kim, J. D. Simeral, L. R. Hochberg, J. P. Donoghue, and M. J. Black, "Neural control of computer cursor velocity by decoding motor cortical spiking activity in humans with tetraplegia," *J Neural Eng*, vol. 5, pp. 155–476, 2008.
[5] A. B. Schwartz and D. W. Moran, "Motor cortical activity during drawing movements: Population representation during spiral tracing," *J Neurophysiol*, pp. 2693–2704, 1999.
[6] W. Wu, Y. Gao, E. Biennenstock, J. P. Donoghue, and M. J. Black, "Bayesian population decoding of motor cortical activity using a Kalman filter," *Neural Comput*, vol. 18, pp. 80–118, 2006.
[7] P. Nuyujukian, V. Gilja, C. A. Chestek, J. P. Cunningham, J. M. Fan, B. M. Yu, S. I. Ryu, and K. V. Shenoy, "Generalization and robustness of a continuous cortically-controlled prosthesis enabled by feedback control design," in *2010 Neuroscience Meeting Planner*. San Diego, CA: Society for Neuroscience, 2010. Program No. 20.7, online.
[8] W. Wu, J. E. Kulkarni, N. G. Hatsopoulos, and L. Paninski, "Neural decoding of hand motion using a linear state-space model with hidden states," *IEEE Trans Neural Rehabil Eng*, vol. 17, pp. 370–378, 2009.